# AN EXPERIMENTAL INVESTIGATION INTO THE RELATIONSHIP BETWEEN INTRALAMINAR CRACK GROWTH AND DELAMINATION

D. Mortell[1], D.A. Tanner[1], C.T. McCarthy[1*]

[1]*Material and Surface Science Institute, Department of Mechanical, Aeronautical and Biomedical Engineering, University of Limerick, Ireland*
**Conor.McCarthy@ul.ie*

**Keywords:** Carbon Fibre; Microtest; SEM; Bending.

## Abstract
*Five carbon/epoxy (HTA/6376) laminates were produced with varying layup orientations. Three and four-point bend tests were carried out under Scanning Electron Microscope (SEM) with an in-situ micromechanical tester during a preliminary test series. The SEM was used to follow the growth and propagation of cracks within the matrix on the micro-scale during testing. The stresses within the specimens under bending load were analysed theoretically in order to calculate the stresses in the primary material directions. It was found that pure bending resulted in significantly higher performance of the laminates tested, indicating the negative effects of shear stress on the laminate failure.*

## 1 Introduction
Composite laminates exposed to significant bending moments can fail from a variety of mechanisms, such as damage and cracking on the micro-scale leading to full delamination, seriously degrading the integrity of the structure. Treating the interlaminar crack growth (i.e. delamination) as a separate damage mechanism to intralaminar crack growth (i.e. matrix cracking, fibre failure) is a drawback of current generation continuum damage models. Matrix cracks propagating towards ply boundaries and leading to micro and macro-scale delaminations demonstrate the lack of independence between these two damage mechanisms.

This study will investigate the effects of shear stress on the intralaminar crack growth leading to delamination. The main focus will be on testing using three and four-point bend testing apparatus. The different types of bending induce alternative stress states in the laminates, leading to conclusions on the influence of shear stress on delamination. The testing will also investigate the effects on varying thicknesses of 90˚ plies in the centre of the laminates which have 0˚ plies on the exterior. Failure of specimens in three-point bending occurs at the middle of the specimen and is due to shear stress. Failure of specimens in four-point bending is due to pure bending stress, experiencing a constant bending moment between the two centre loading pins [1].

## 2 Description of Analysis

This section will clarify the details of the material used as well as the processes of the testing procedure and conventions observed.

### *2.1 Material Properties*

The material used during testing was HTA/6376 and its properties are listed in Table 1.

| ***Property*** | ***$E_{11}$ (GPa)*** | ***$E_{22}$ (GPa)*** | ***$G_{12}$ (GPa)*** | ***$v_{12}$*** | ***Ply Thickness (mm)*** |
|---|---|---|---|---|---|
| ***Value*** | 140 | 10 | 5.2 | 0.3 | 0.125 |

**Table 1.** Material Properties for HTA/6376

### *2.2 Laminate Orientations*

Five different laminates were produced to provide specimens for testing. The layup orientations and justifications can be seen in Table 2.

| ***Fibre Orientation*** | ***Justification*** |
|---|---|
| $[90_{10}]$<br>$[90_4/0_7/90_4]$ | For general benchmarking, crack growth analysis,<br>and comparison with existing literature [2] |
| $[0_4/90_3/0_4]$<br>$[0_4/90_7/0_4]$<br>$[0_4/90_{11}/0_4]$ | To investigate the effect of increasing the<br>thickness of the 90˚ plies at the core of the laminate |

**Table 2.** Laminate fibre orientation and justification

Preliminary testing for the purposes of this paper consisted in focussing the analyses on three and four-point bend testing of the following specimens. The specimen ID is used to identify the specimens of different layup orientation in the results section. Dimensions associated with specimens tested can be seen in Figure 1.

| ***Layup Orientation*** | ***Specimen ID*** | ***No. of 3-point Tests.*** | ***No. of 4-Point Tests*** |
|---|---|---|---|
| $[90_4/0_7/90_4]$ | **4.x** | 4 | 4 |
| $[0_4/90_7/0_4]$ | **5.x** | 3 | 3 |
| $[0_4/90_3/0_4]$ | **2.x** | 4 | 4 |

**Table 3.** Number of tests conducted and specimen identification

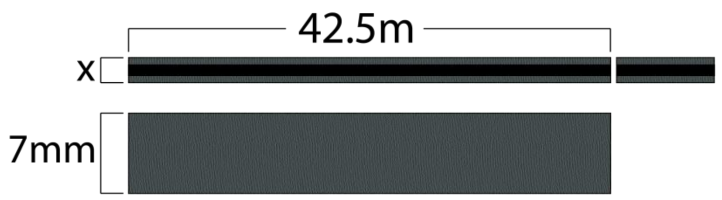


**$[90_4/0_7/90_4]$** x = 1.875mm
**$[0_4/90_7/0_4]$** x = 1.875mm
**$[0_4/90_3/0_4]$** x = 1.375mm

**Figure 1.** Dimensions from specimen sets 4,5 & 2

### *2.3 Microtester Crossheads*

The three and four-point crossheads for the microtester can be seen in Figure 2, (A) and (B) respectively. The centre of the outermost pins on both sets of crossheads are 35mm apart. The specimens in Figure 2 represent the typical failure of specimens in three and four-point bending.

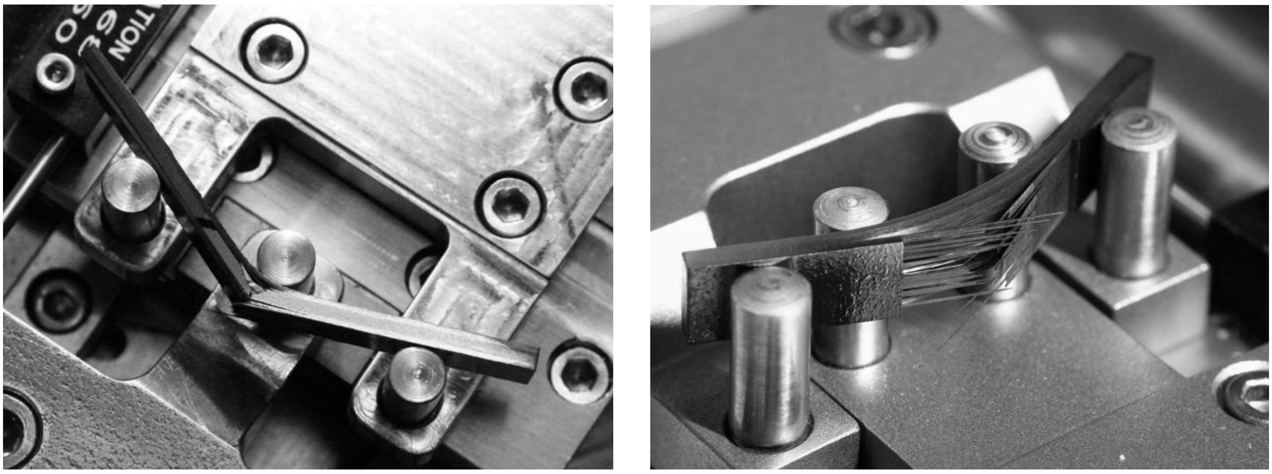

**(A)** **(B)**

**Figure 2.** 3-point bend example (A), and 4-point bend example (B) exhibiting typical failure

*2.4 General Testing Procedure*

The specimens were preloaded in the microtester to approximately 10N to prevent the specimen from sliding along the pins. After inserting in to the evacuated SEM chamber, a displacement of 0.033mm/min was applied. Video streaming from the SEM was recorded to be reviewed at a later stage to relate crack behaviour/propagation at any moment of time with the load being applied at that instance.

## 3 Theoretical Analysis

Knowing which layers in a laminate see the highest stresses while the laminate is undergoing bending is important in both predicting and explaining crack initiation and propagation, originating from interface decohesion on the micro-scale at the locations of highest stress. The coordinate system used for the specimens analysed in this study can be seen in Figure 3.


**Figure 3.** Typical specimen and coordinate system

It is assumed in classical laminate theory [3] that the stresses in the *xy*-plane dominate the behaviour of the plate under loading conditions. It is assumed that an approximate state of plane stress exists which is only influenced by $\sigma_x$, $\sigma_y$, and $\tau_{xy}$ and that $\sigma_z$, $\tau_{xz}$, and $\tau_{yz}$ are assumed to be zero. This would suggest that calculating the stresses in the *x* and *y* directions would be of greatest importance to the theoretical analysis of a test specimen. The constitutive equation gives resultant forces and moments as functions of in-plane strains and their curvatures. In order to calculate the value of in plane strains and curvatures, the ABD matrix from the constitutive equation must be inverted so as to produce:

$$\begin{bmatrix} \varepsilon^0{}_{xx} \\ \varepsilon^0{}_{yy} \\ \varepsilon^0{}_{xy} \\ k_x \\ k_y \\ k_{xy} \end{bmatrix} = \begin{bmatrix} A_{11} & A_{12} & A_{16} & B_{11} & B_{12} & B_{16} \\ A_{12} & A_{22} & A_{26} & B_{12} & B_{22} & B_{26} \\ A_{16} & A_{26} & A_{66} & B_{16} & B_{26} & B_{66} \\ B_{11} & B_{12} & B_{16} & D_{11} & D_{12} & D_{16} \\ B_{12} & B_{22} & B_{26} & D_{12} & D_{22} & D_{26} \\ B_{16} & B_{26} & B_{66} & D_{16} & D_{26} & D_{66} \end{bmatrix}^{-1} \begin{bmatrix} N_x \\ N_y \\ N_{xy} \\ M_x \\ M_y \\ M_{xy} \end{bmatrix} \quad (1)$$

Using strain and curvature results from Eq.1, $\sigma_{xx}$, $\sigma_{yy}$ and $\sigma_{xy}$ can be calculated for each individual layer of a laminate using Eq.2, and represent the stresses in the *xy*-plane.

$$\begin{bmatrix} \sigma_{xx} \\ \sigma_{yy} \\ \sigma_{xy} \end{bmatrix}_k = \begin{bmatrix} Q'_{11} & Q'_{12} & Q'_{16} \\ Q'_{12} & Q'_{22} & Q'_{26} \\ Q'_{16} & Q'_{26} & Q'_{66} \end{bmatrix}_k \begin{bmatrix} \varepsilon^0{}_{xx} \\ \varepsilon^0{}_{yy} \\ \varepsilon^0{}_{xy} \end{bmatrix} + \begin{bmatrix} Q'_{11} & Q'_{12} & Q'_{16} \\ Q'_{12} & Q'_{22} & Q'_{26} \\ Q'_{16} & Q'_{26} & Q'_{66} \end{bmatrix}_k \begin{bmatrix} k_x \\ k_y \\ k_{xy} \end{bmatrix} \quad (2)$$

Where the *Q'* matrix is the reduced stiffness matrix of the particular layer in question, *k*.

A MATLAB script was written to calculate the stresses in the laminate based on the results achieved during testing. Figure 4 shows the distribution of stress in the *x* direction through the thickness of the laminate. The laminate used in this example is $[0_4/90_7/0_4]$ under the maximum recorded three-point bending load of 1kN which specimen 5.3 failed at.

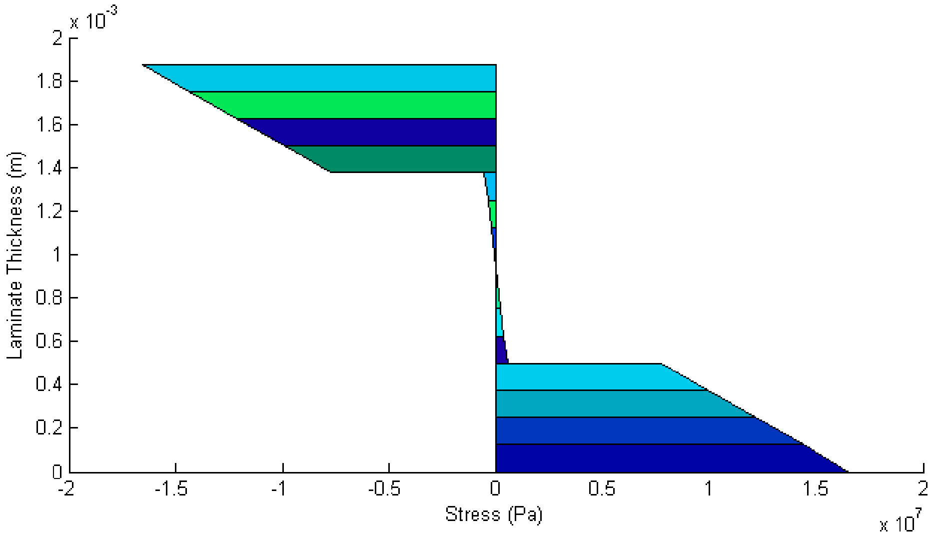


**Figure 4.** Variation of $\sigma_{xx}$ through laminate thickness

Due to the specimen being bent along its *x*-axis it is most relevant to view the normal stresses between the plies in the *x*-direction as they are two orders of magnitude higher than the comparable stresses in the *y*-direction. The figure highlights the effect of the particular stacking sequence being investigated in this example.

Observation of classical lamination theory, such as the assumption that the behaviour of a laminate is only influenced by $\sigma_x$, $\sigma_y$ and $\tau_{xy}$, can lead to inaccuracies when predicting some of the stresses that actually cause the failure of composite material. Interlaminar stresses are one of the failure mechanisms uniquely characteristic of composite materials [3].

In the case of a beam under three- point bending [4], the interlaminar shear stress $\sigma_{xz}$ is given by the following equation.

$$\sigma_{xz}^{k} = -a_{xx}^{k}\tau_{0}\left[4\left(\frac{z}{h}\right)^{2} + d_{k}\right] \tag{3}$$

Which is used to calculate the shear stresses associated with each individual ply, *k*, under load *P*, at distance *z* from the neutral axis to the upper and lower surfaces of each ply within the laminate which are at a distance *h* apart, with

$$\tau_{0} = -\frac{3P}{4bh} \tag{4}$$

and

$$a_{xx}^{k} = \left(Q_{11}^{k}D_{11}^{*} + Q_{12}^{k}D_{12}^{*} + Q_{16}^{k}D_{16}^{*}\right)\left(\frac{h^{3}}{12}\right) \tag{5}$$

Where $d_k$ is a constant applied to each ply to assure continuity of $\sigma_{xz}$ from layer to layer, and that shear stress is zero on the upper and lower surfaces of the laminate. The transverse shear stress of a beam of homogenous material properties can be calculated using

$$\sigma_{xz}^{k} = \tau_{0}\left[1 - 4\left(\frac{z}{h}\right)^{2}\right] \tag{6}$$

The transverse shear stress is plotted in Figure 5 using loading information and material properties from the three-point bend test subjected to specimen 5.3.

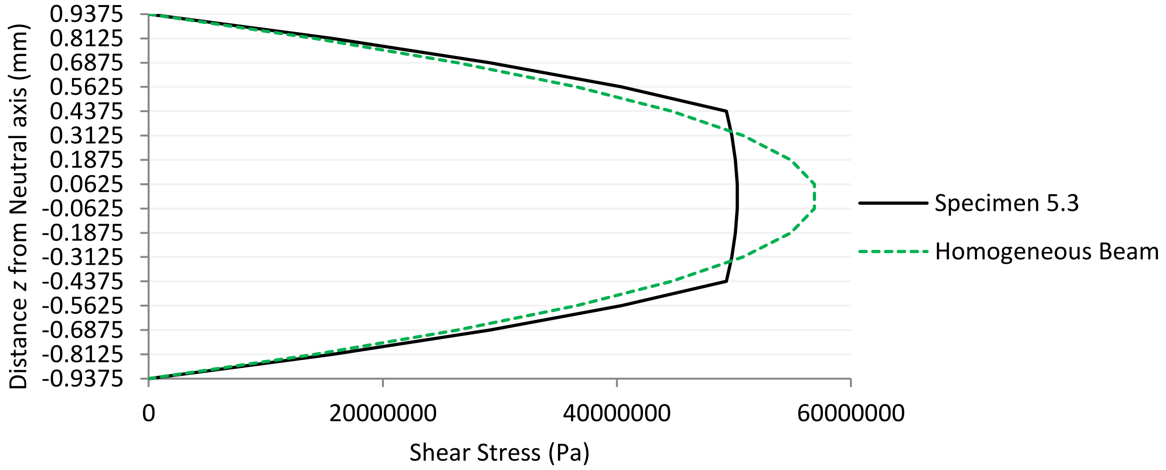


**Figure 5.** Variation of the shear stress across the laminate for Specimen 5.3 loaded to 1kN

The influence of the stacking sequence upon the transverse shear stress can be observed when compared to the shear stress in a comparable homogenous beam.

## 4 Results

The results from three and four-point bend tests are presented and discussed below.

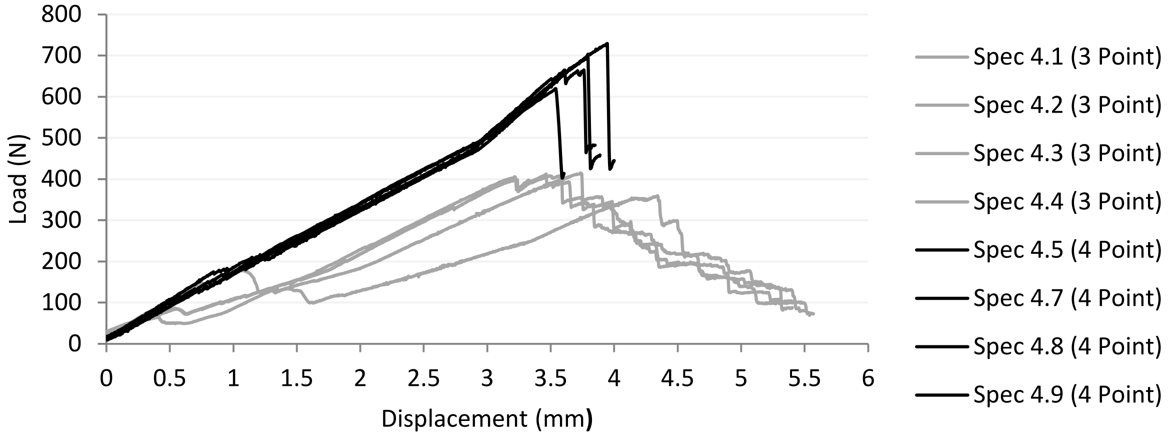


**Figure 6.** $[90_4/0_7/90_4]$ 3 & 4-point bending

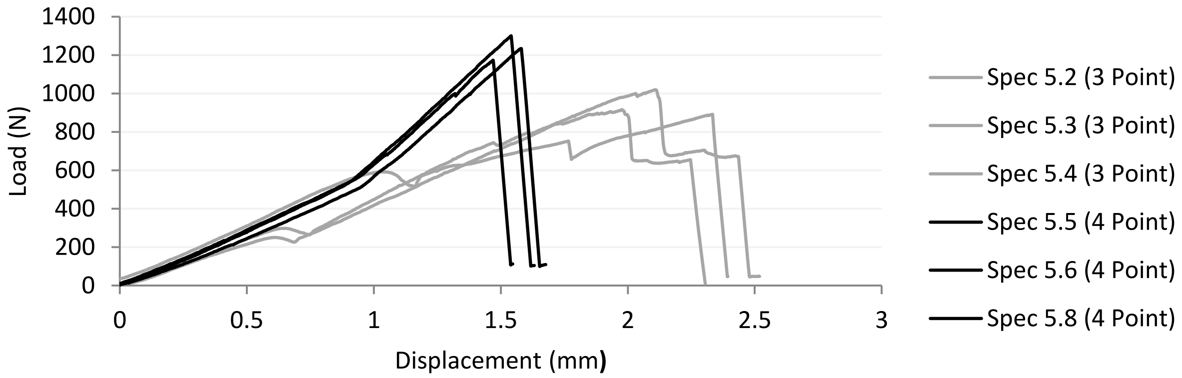


**Figure 7.** $[0_4/90_7/0_4]$ 3 & 4-point bending

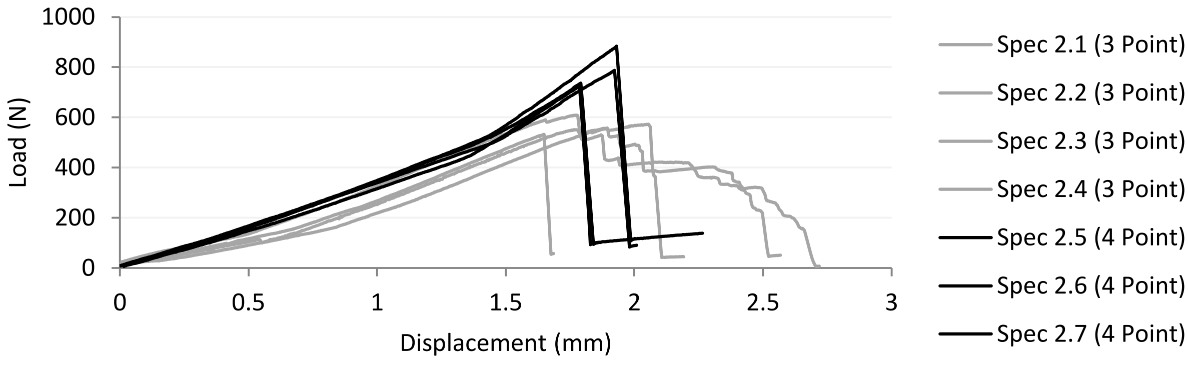


**Figure 8.** $[0_4/90_3/0_4]$ 3 & 4-point bending

Figures 6,7 and 8 highlight the difference between the manner in which the material performs while being loaded in three or four-point bending, and that the behaviour was consistent. The load bearing capacity of each of the specimens improved in four-point bending.

| *Layup Orientation* | *Avg. 3-Point (N)* | *Avg.4-Point (N)* | *% Difference* |
|---|---|---|---|
| $[90_4/0_7/90_4]$ | 393 | 672 | 71% |
| $[0_4/90_7/0_4]$ | 936 | 1223 | 31% |
| $[0_4/90_3/0_4]$ | 559 | 772 | 38% |

**Table 4.** Average 3 & 4-point bending results for all specimens tested

Crack growth was studied in a number of specimens. The images in Figures 9 and 10 show crack formation and delamination as characteristically seen in specimens with 90˚ fibres on the outside, as seen in Figure 9, and then at the core of the specimen, Figure 10. The dashed boxes in (B) indicate the location of viewing for the corresponding image on the left (A).

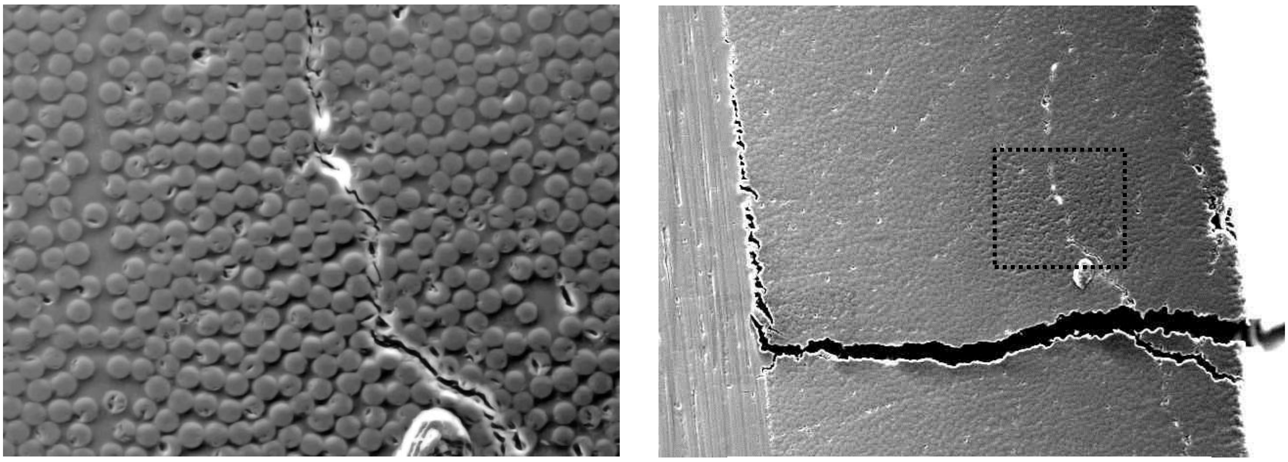

(A) (B)

**Figure 9.** Crack growth (A) prior to significant intralaminar crack growth leading to delamination of specimen 4.3

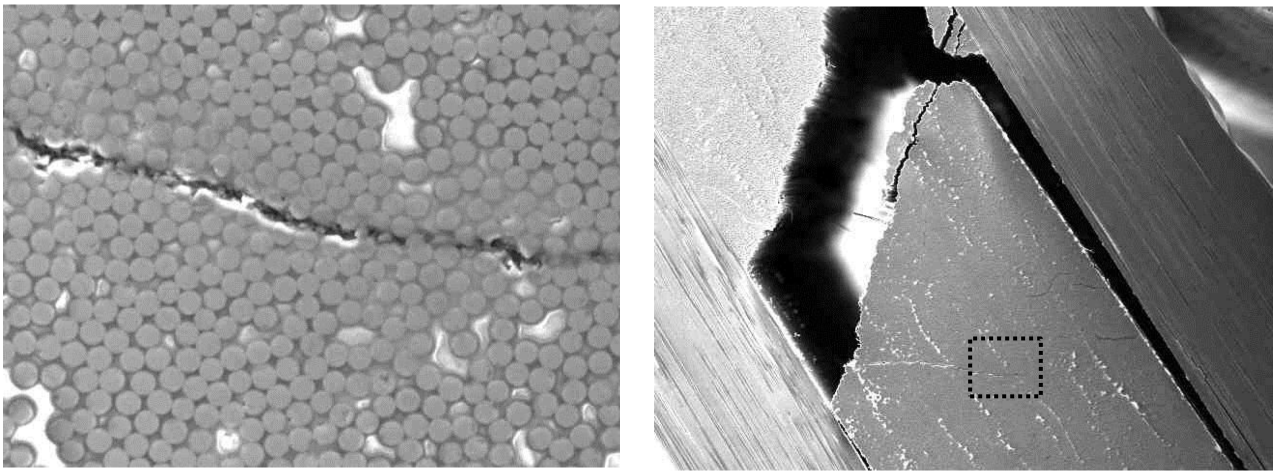

(A) (B)

**Figure 10.** Crack growth (A) prior to significant intralaminar crack growth leading to delamination of specimen 5.5

During testing, there tended to be a trend of having two stages of failure. The 90˚ fibres would tend to fail first, regardless of whether they were located on the outside or at the core of the specimen. This would then be followed at a higher load by the 0˚ fibres which would result in complete failure of the specimen. Images (A) from Figures 9 & 10 were locations identified as potentially leading to significant crack growth before the actual cracking seen in images (B) of Figures 9 & 10.

## 5 Conclusions & Further Testing

It was shown that the performance of each of the laminates increased when under four-point bending conditions, therefore eliminating shear stress as a factor. This indicates that further research should be conducted into the effects of shear on the crack propagation and delamination of a laminate. When 90˚ plies were located at the core of the specimen, it was shown that by reducing the 90˚ plies from 7 layers to 3 layers, a 57% reduction in thickness, that in three and four-point bending the average maximum load achieved was reduced by 41% and 37% respectively. Further testing will include asymmetric four-point bending, which can be used to calculate interlaminar shear stress [5] in conjunction with Equation 4.

## Acknowledgements

This work was funded by the Science Foundation of Ireland.

## References

[1] Khashaba U.A., Seif M.A., Effect of different loading conditions on the mechanical behaviour of $[0/\pm 45/90]_s$ woven composites, *Composite Structures*, **74**, pp. 440-448 (2006).

[2] Canal L.P. et al., Intraply fracture of fibre-reinforced composites: microscopic mechanisms and modelling, *Composites Science and Technology*, Available online 21 April 2012, ISSN 0266-3538, 10.1016/j.compscitech.2012.04.008.

[3] Jones R.M., *Mechanics of Composite Materials*. Taylor & Francis, USA, pp. 210-242 (1975).

[4] Berthelot J., *Composite Materials – Mechanical Behaviour and Structural Analysis*. Springer Verlag, New York (1999).

[5] Yoshihara H., Interlaminar shear strength of medium-density fibreboard obtained from asymmetrical four-point bending tests, *Construction and Building Materials*, **34**, pp. 11-15 (2012).